JOURNAL OF MATERIALS SCIENCE 20 (1985) 1586–1601

Solution crystallization of polyethylene at high temperatures

Part 2 *Three-dimensional crystal morphology and melting behaviour*

S. J. ORGAN, A. KELLER
HH Wills Physics Laboratory, University of Bristol, Tyndall Avenue, Bristol, UK

The three-dimensional morphologies and melting behaviour of crystals grown from various solvents at temperatures between 93.0 and 112.8° C have been studied. These crystals cover a range of lateral habits, with axial ratios from 1.60 to 3.00 and varying degrees of prism face curvature. Electron diffraction revealed two distinct types of crystal, usually present in roughly equal proportions. Sectorization could be distinguished in all preparations, although the sectors became less well defined as the axial ratio increased with concomitant development of curving prism faces. This was confirmed by both paraffin decoration and melting behaviour. Preferential sector melting was seen in only one sample type. Crystals with the larger axial ratios showed more uniform melting behaviour and also a reduced tendency to anneal on heating. Possible explanations for the observed trends are discussed, and in particular the loss of directionality of the fold depositions with development of prism face curvature is commented on with relevance to the underlying mechanism of chain folding.

1. Introduction

This paper is the second in a series of three, serving the broad objectives outlined in the introduction of Part 1 [1]. Single crystals have been grown from solution in a variety of solvents at temperatures up to 120° C. Thus an overlap in the range of absolute crystallization temperature (T_c) accessible for crystallization both from solution and from the melt has been achieved. In Part 1, the lateral habits of the crystals, as seen in two dimensions, were followed, characterized and analysed. For a given molecular weight distribution and solution concentration, the crystal shape was found to depend primarily on the crystallization temperature with only small effects due to solvent. As T_c is raised the crystals become increasingly elongated and their faces show distinct curvature. This raises fundamental questions as to the mechanism of growth of the crystals, as discussed in Part 1.

In the present paper (Part 2) we proceed to examine two further aspects of selected crystals from those described in Part 1: (1) the three-dimensional features of the morphology; and (2) their thermal stability and melting behaviour. Both of these involve the issue of sectorization.

The significance of sectorization is that it defines the fold plane direction and hence provides a record both of the present state of a crystal and its growth history. It tells us the position of the growth front and hence the shape of the crystal at any stage in its development. This is a unique situation in crystal growth which can provide significant information as to the mode of deposition of the polymer chains and the general issue of chain folding.

As is familiar from previous work, the three-dimensional nature of the crystal morphology, (1) above, is a direct consequence of sectorization. As such it can serve as an identification of sectors and their mutual arrangements and can provide information on the way the crystals have grown.

0022–2461/85 $03.00 + .12

Figure 1 Single crystal of polyethylene grown from 0.05% solution in octane at 93° C. The central pleats indicate that the crystal has collapsed from its original three-dimensional structure (× 7800).

The three-dimensional morphology of a selection of crystals has been investigated here using electron diffraction effects. In addition, a sensitive decoration technique involving the vacuum deposition of thermally degraded polyethylene onto the crystal surface [2] has been used as a further indication of the nature of the sectorization.

The thermal behaviour, (2) above, has a dual function in the present work. Firstly, differential sector melting offers another method of identifying sectors – complementing those mentioned above. Secondly, the melting point is a measure of both the fold length and the lattice perfection, and thus has a significance beyond that related to sectorization.

First we shall briefly review the evidence of sectorization as manifest by three-dimensional crystal morphology. Fig. 1 shows a typical single crystal of polyethylene. It is obvious from the central pleat that the crystal did not grow flat, but has collapsed on sedimentation. Collapse can occur by shear of molecular chains parallel to the *c* axis, or by tilting each sector so that it lies flat on the substrate, or by a combination of these two mechanisms. The three-dimensional structures of polyethylene crystals grown from xylene and octane at temperatures below 100° C are well documented. Fig. 2 shows the principle habits of lozenge and slightly truncated lozenge shaped crystals. For the simplest structures, as in Fig. 2a and c, the basal planes bound by the {1 1 0} faces are found to be close to {3 1 2} [3] with a maximum slope of 29° (although subsequent work [4] suggests that this index is not always strictly adhered to). The ridged lozenge, Fig. 2d, and the chair crystal, Fig. 2b, are common variants of the simple forms. The chair morphology, which has not been given much attention since its original recognition, will be further discussed later.

Kawai and Keller [5] have studied more highly truncated crystals grown from octane at temperatures between 80 and 100° C and considered the compatibility of the different sector obliquities. An optimum truncation ratio for the smooth joining of {3 1 2} and {2 0 1} or {3 1 4} and {1 0 1} surfaces was calculated. Most of the crystals grown had truncation ratios close to the optimum figure, but the influence of increasing truncation ratio, which competes with that of smooth sector joining of the facets with the favoured obliquities as the crystallization temperature is raised, was also apparent. As the crystals become more elongated the obliquities of one or both sets of crystal faces will have to deviate from the calculated values in order to achieve smooth joining. The three-dimensional structures of more elongated crystals grown at higher temperatures are less well-defined. Keith [6], studying crystals grown in thin films from n-octadecane and n-dotriacontane, found ridged structures rather different from those seen in the simple pyramidal crystals of Fig. 2. At relatively low crystallization temperatures ridges parallel to ⟨1 5 0⟩ were seen and the crystals were best described by (5 1 6) (1 1 0) and (1 0 1) (1 0 0) type faces. At higher temperatures, where the axial ratio of the crystals exceeded about 2, a new habit was observed where [0 1 0] ridges appeared along the full length of the crystal. Khoury and Bolz [7] have examined the chain orientation in highly elongated crystals grown from dodecanol at 115° C. In most cases they found that all the chains in the crystal were inclined in the same sense from the vertical. The angle of tilt was about 34° in the central portion and decreased gradually to 22° at the crystal edges.

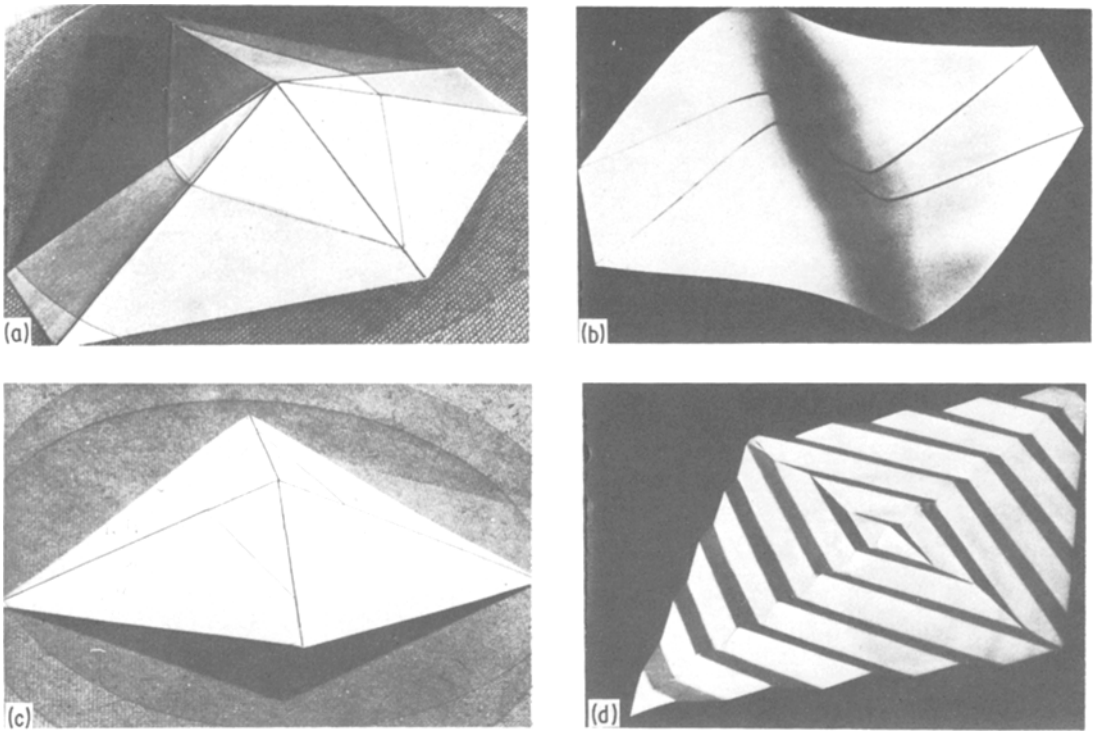

Figure 2 Principal three-dimensional habits of simple polyethylene crystals. (a) Truncated hollow pyramid. (b) Chair crystal. (c) Hollow pyramid. (d) Corrugated crystal. (After Bassett, *et al.* [3]).

Both these results suggest new types of crystal structure, the details of which are not clear.

The distinct sectors which are apparent in lozenge and truncated lozenge type crystals arise as a consequence of chain folding along preferred crystallographic directions and are directly related to the three-dimensional crystal structures. Since the shapes of crystals grown at higher temperatures are not bounded by crystallographic planes, and indications of rather different three-dimensional forms have been seen, sectorizaton is no longer an obvious implication. Sectorization can be demonstrated in a variety of different ways. In this paper dark-field electron microscopy (EM), paraffin decoration, and examination of crystal melting behaviour are used to investigate the presence of sectors in various types of crystal. Differences in chain orientation within crystals can be detected using the dark-field technique and provide useful information as to the original structure of the crystals. The method consists of selecting a particular diffraction spot and viewing the image of the parts of the crystal which give rise to that reflection. If the crystal is tilted, various sectors will successively appear bright, as the relevant planes are brought into a diffracting position. By measuring the tilt angles at which different areas become bright, the relative orientations of diffracting planes within the crystal can be found.

Decoration techniques can detect sectorization by revealing variations in the surface structure of the crystals. Gold decoration has been used in the past with some success [8], but more striking is the polyethylene evaporation method developed by Wittman and Lotz [2], which has been applied to two preparations here.

2. Experimental procedure

A selection of crystals exhibiting a range of morphologies were chosen for investigation. The crystals were all grown from 0.05% w/v solution of Rigidex 50 linear polyethylene in various solvents. Details of their preparation are reported in Part 1 [1]. The following abbreviations are used throughout this paper to describe the samples studied:

(a) O 95.0 Crystals grown from octane at 95.0° C

(b) EC 102.5 Crystals grown from ethyl caproate at 102.5° C

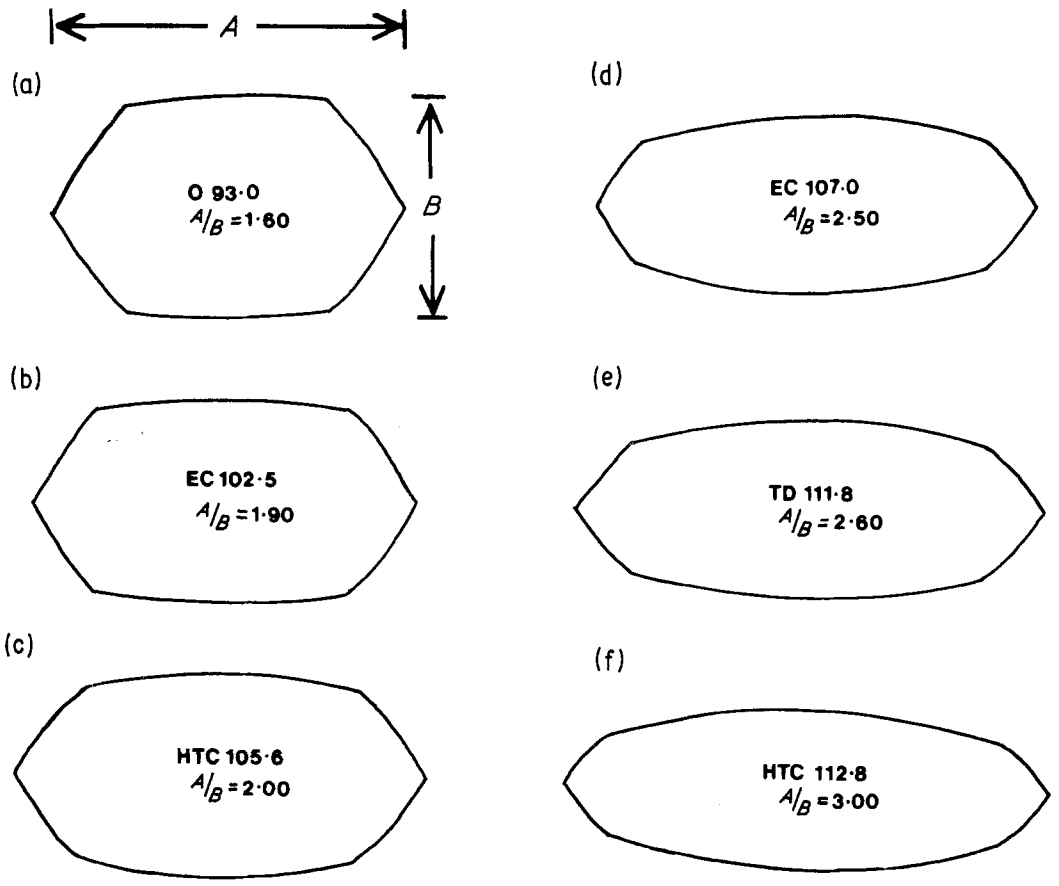

Figure 3 Typical crystal morphologies for the preparations studied. The abbreviations used are defined in the text.

(c) HTC 105.6 Crystals grown from hexatriacontane at 105.6° C

(d) EC 107.0 Crystals grown from ethyl caproate at 107.0° C

(e) TD 111.8 Crystals grown from tetradecanol at 111.8° C

(f) HTC 112.8 Crystals grown from hexatriacontane at 112.8° C.

These particular preparations were selected to cover a range of axial ratios between 1.60 and 3.00 and show varying degrees of curvature. For reference the "typical crystal" morphology (as described in Part 1) for each case is illustrated in Fig. 3. Samples (b), (c), (e) and (f) were used for dark-field EM. The structure of crystals of type (a) is well established [5]. Crystals from (d) were too small to be investigated by this technique. Samples (a), (c), (d), (e) and (f) were used for melting studies. Crystals of type (b) tended to be highly multilayered, which made them less suitable for this purpose. Two samples were decorated with evaporated polyethylene. The first was similar to (a), but with $T_c = 95.8°$ C, the second was prepared under identical conditions to (e).

Samples were prepared for dark-field EM as described previously [1], but not shadowed. A tilt-rotate specimen holder was used and the procedure described by Bassett *et al.* [3] followed. A suitable crystal was selected and rotated so that an appropriate set of diffracting planes was parallel to the tilting axis. An image was then obtained using a diffraction spot arising from these planes, and the specimen tilted. The tilt angles at which different parts of the crystal became bright were noted and the image recorded onto specially sensitive film (DuPont "Cronex" medical recording film). Dark-field EM of polymer crystals poses some experimental difficulties due to the gradual destruction of crystallinity by the electron beam. Prolonged exposure to the beam results in reduced tilt angles and eventually in the disappearance of useful diffraction effects. It is necessary to work quickly and at very low levels of illumination. Ideally, large crystals should be

used. Since the crystals studied were not grown specifically for this purpose they were in most cases rather small and, at the levels of illumination required, diffraction effects lasted only a few minutes. In most cases, tilt angles could not be exactly reproduced, indicating that significant beam damage had occurred. Also, due to the limited time available, specimens were not always rotated into exactly the right orientation before tilting. For both these reasons, the tilt angles obtained cannot be regarded as quantitatively accurate, although they do give a good qualitative picture of orientation differences within crystals.

For the decoration, Rigidex 006/60 linear polyethylene ($M_w \simeq 116\,000$, $M_w/M_n \simeq 7.5$) was used. 3 mg of this polymer was heated under vacuum to approximately 280° C, and allowed to evaporate onto crystals lying on carbon films. The decorated crystals were then shadowed with Pt/Pd before examination in the electron microscope.

For the melting studies, two methods were used. One involved direct microscopical observation of crystals in various stages of melting, while the second detected differences in melting temperature by calorimetric means. In the former case a general view of the melting behaviour of the crystals and a rough value for the melting temperature were first obtained by heating crystals deposited onto a glass slide on a Koffler hotbench. The slide was positioned so that the temperature varied from about 100 to 150° C across its length. After 15 min it was removed and examined in the phase contrast microscope. The temperature range over which melting occurred was identified from the positions on the slide where crystals showed the first signs of melting and where they had completely melted. Crystals in the intermediate region were carefully studied for signs of preferential sector melting.

Samples were prepared for electron microscopy in one of two ways. In some cases crystals which had been heated on a glass slide were coated with carbon, and subsequently detached. Alternatively, crystals were deposited onto carbon coated specimen grids which were then held for 15 min at various temperatures within the melting range in a Mettler hot stage. The samples were then shadowed with Pt/Pd to improve contrast. The latter method generally proved more satisfactory and allowed for more accurate temperature determination.

For calorimetric analysis samples were prepared as follows. A small amount of each crystal preparation, in suspension in xylene or octane, was mixed with a few drops of silicone oil. The solvent was removed by warming the mixture slightly under vacuum for several hours, thus leaving the crystals suspended in silicone oil. For good thermal contact it is important that the crystals should not be allowed to dry before the silicone oil is added, otherwise voids and clumped lamellae may result. Drops of the crystal suspensions were sealed into sample pans and heated in a Perkin-Elmer DSC 2 differential scanning calorimeter. Conditions were optimised to give the best resolution of the melting endotherms. In most cases a heating rate of $5°\,C\,min^{-1}$ proved satisfactory. As very small amounts of crystal were present (~ 0.05 mg) a high sensitivity range of 0.1 to 0.2 $mcal\,sec^{-1}$ was used. Variations in peak position with heating rate were not investigated, since it is differences in melting points, rather than absolute values, which are of interest. Traces were calibrated using an indium standard.

3. Results

3.1. Dark-field EM

In most cases dark-field EM revealed two distinct types of crystal within each sample. These will be referred to as types A and B. In a type A crystal different parts of the crystal became bright for different senses of tilt. In a type B crystal the whole crystal could be made to light up successively using one sense of tilt, while for the other sense the crystal remained dark at all tilt values. Types A and B are analogous to the hollow pyramid and chair type crystals respectively, shown in Figs. 2a and b. The crystals have a similar structure, but the two crystal halves have joined in different ways.

Table I gives a summary of the results. The tilts quoted are the angles through which the specimen was rotated to produce maximum brightness in a particular area. In the majority of cases the two types of crystal were present in roughly equal proportions, although no type B crystals were found in the sample TD111.8. Type A crystals showed some signs of sectorization in all cases, although the distinction between different sectors became less pronounced for crystals with larger axial ratios. Fig. 4 shows two examples of type A crystals from the sample HTC105.6. In the sample HTC112.8, which had the most extreme value of axial ratio, some evidence of sectorization was

TABLE I Dark-field electron microscopy results

Sample	Number of crystals		Imaging diffraction	Type A		Type B	
	Type A	Type B		Tilt in 1 1 0 sectors	Tilt in 1 0 0 sectors	Tilt in centre	Tilt at sides
EC102.5	5	5	1 1 0	16–28°	12–20°	0–3°	12–20°
HTC105.6	8	7	1 1 0	18–25°	10–15°	0–5°	8–12°
			2 0 0	19–24°	30°	25–34°	16–22°
TD111.8	–	12	1 1 0	–	–	0–6°	10–20°
HTC112.8	6	4	1 1 0	Sectors not well defined, see text.		–	–
			2 0 0			20–30°	10–15°

seen but the form this took was variable. Fig. 5 shows two examples of type A crystals from the sample HTC112.8. The crystal in Figs. 5a to e appears to be roughly divided into four sectors, diametrically opposed sectors diffracting at similar but opposite tilt values. The crystal in Figs. 5f to i, however, shows indications of the more usual six-sectored structure. Other crystals showed a distinction down the centre of the crystal, but no obvious sectorization within the two crystal halves. Tilt values were very variable, but some representative values are shown on the diagram. In type B crystals, any distinction between different sectors was rare. The usual structure of these crystals was a central portion, roughly parallel to [0 1 0], bounded by two regions of equal tilt along the two long sides of the crystal. Fig. 6 shows examples of type B crystals from the samples

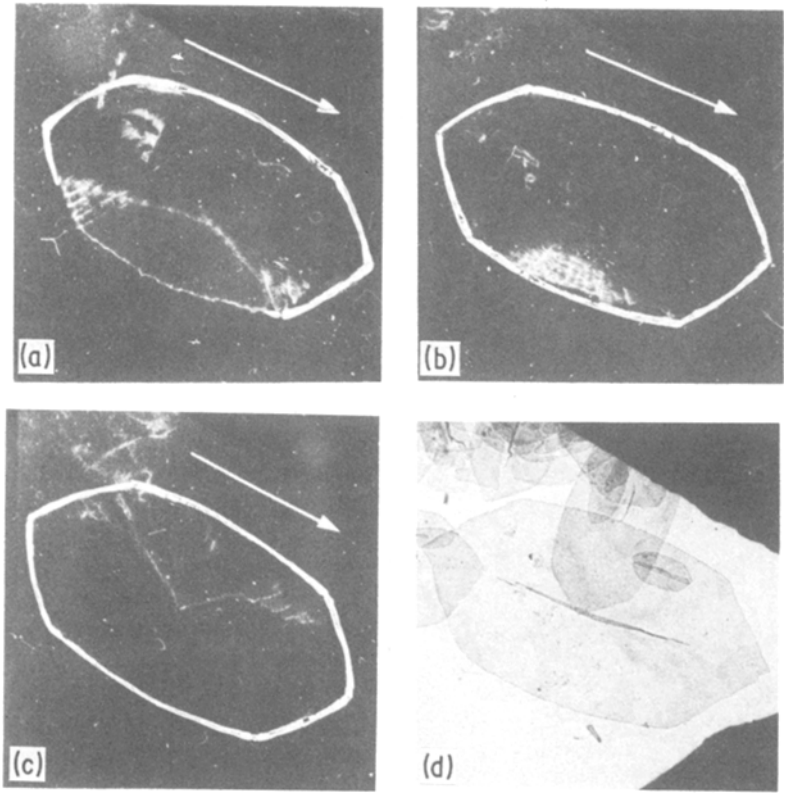

Figure 4 Dark and bright field electron micrographs of crystals grown from hexatriacontane at 105.6° C. Tilting series with tilt axes as shown by arrows. (a) to (c) were imaged with 2 0 0, (e) to (h) with 1 1 0. Tilt angles are as follows: (a) − 23°, (b) − 30°, (c) + 19°, (d) BF, (e) − 13°, (f) + 19°, (g) + 15°, (h) − 21°, (i) BF. Crystal outlines have been added in white.

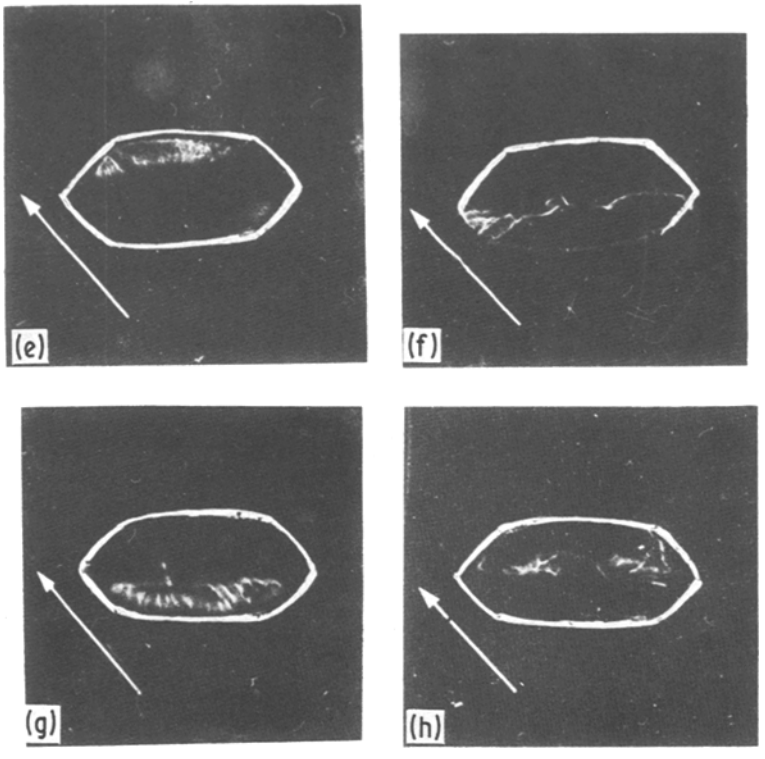

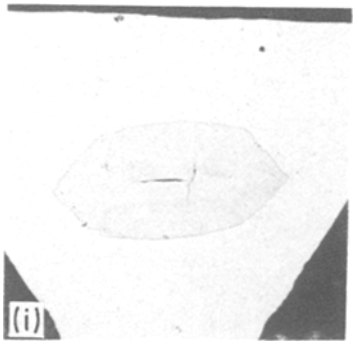

Figure 4 Continued.

HTC105.6 and TD111.8. The results indicate a higher chain tilt in the central region of the crystal, which is gradually reduced towards the crystal edges. These crystals may be regarded as extreme examples of the chair type crystal, where the distortion produced by joining the two non-matching crystal halves is sufficient to remove any evidence of sectorization. However, it should be pointed out that the chair-type crystal, exhibiting as it does a distinct central region, is only realistic in combination with sectorization. If the chain tilt was uniform throughout each of the crystal halves, smooth joining would be possible and no central discontinuity would be seen.

3.2. Surface decoration

Fig. 7 shows electron micrographs of the two types of crystal which were decorated with thermally degraded polyethylene. It can be seen that the decoration is randomly oriented on the background carbon film, but shows preferential orientations on the crystal surfaces. The direction of preferential orientation varies across the crystals and sector boundaries can be seen as sudden changes in orientation. Crystals of the type shown in Fig. 7a, grown from octane at 95.8° C, show six distinct sectors as reported previously [2]. Well defined sector boundaries are clearly revealed by the decoration. Different sectors can also be distinguished in the crystals grown from tetradecanol at 111.8° C, as illustrated in Fig. 7b. The smaller size of these crystals should be taken into account, but examination of the pattern of decoration shows a more gradual change in orientation over the crystals, in contrast to the sharp discontinuities seen at the sector boundaries in Fig. 7a. For the crystals grown from octane, the direction of orientation of the decoration is principally along [0 1 0] and [1 1 0] in the (1 0 0) and (1 1 0) sectors respectively. In the crystals grown from tetradecanol, the principal orientation of the decoration within the

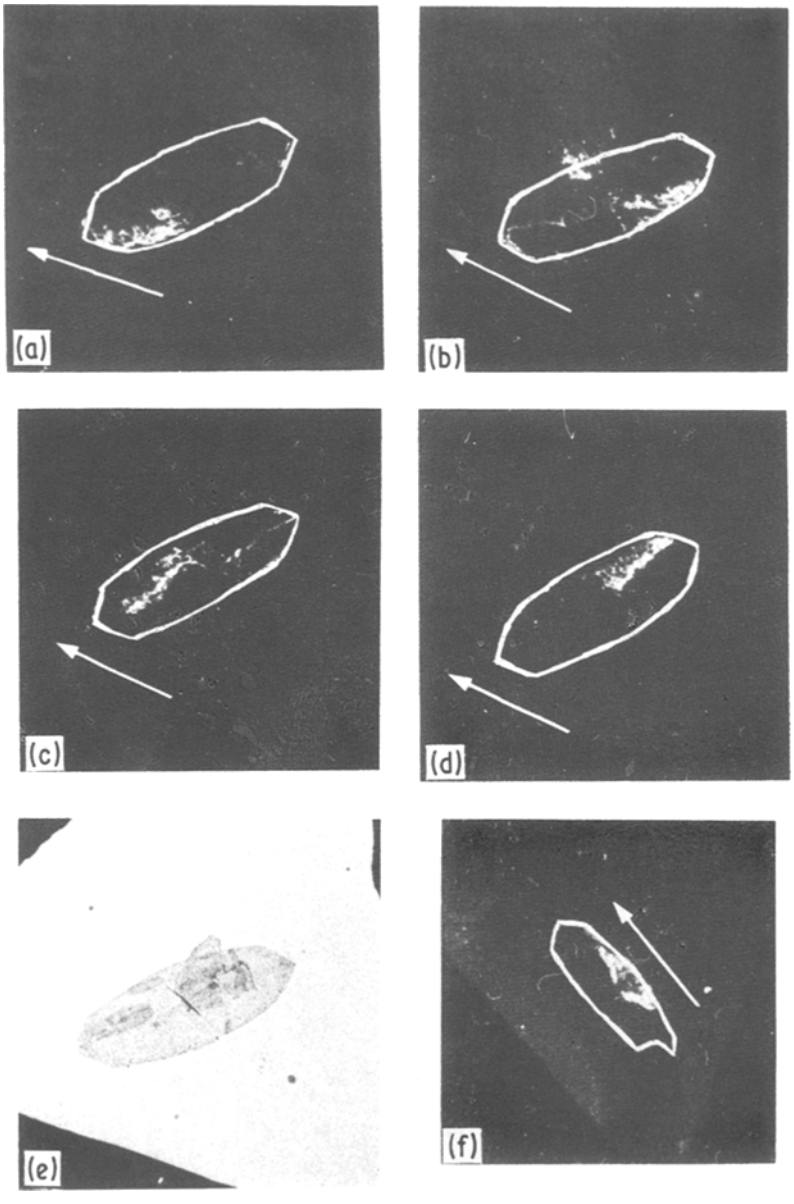

Figure 5 Dark- and bright-field electron micrographs of crystals grown from hexatriacontane at 112.8° C. Tilting series with tilt axes as shown by arrows. (a) to (d) are imaged with 1 1 0, (f) to (h) with 2 0 0. Tilt angles are as follows: (a) + 24°, (b) + 15°, (c) − 22°, (d) − 30°, (e) BF, (f) + 28°, (g) + 22°, (h) − 26°, (i) BF. Crystal outlines have been added in white.

"1 0 0" sectors varies within the sector, deviating more from [0 1 0] as the sector boundaries are approached.

3.3. Crystal melting

Figs. 8 to 12 show electron micrographs of crystals in various stages of melting, for the preparation O 95.0, HTC 105.6, EC 107.0, TD 111.8 and HTC 112.8. Also included in the figures are the corresponding differential scanning calorimetry (DSC) traces, showing the melting endotherms of the crystals suspended in silicone oil.

In Fig. 8, relating to the sample O 95.0, the DSC thermogram shows three distinct peaks, occurring at 125.7° C, 126.6° C and 130.5° C. The third, broader peak is generally assumed to correspond to the melting of material which has thickened during heating by some annealing

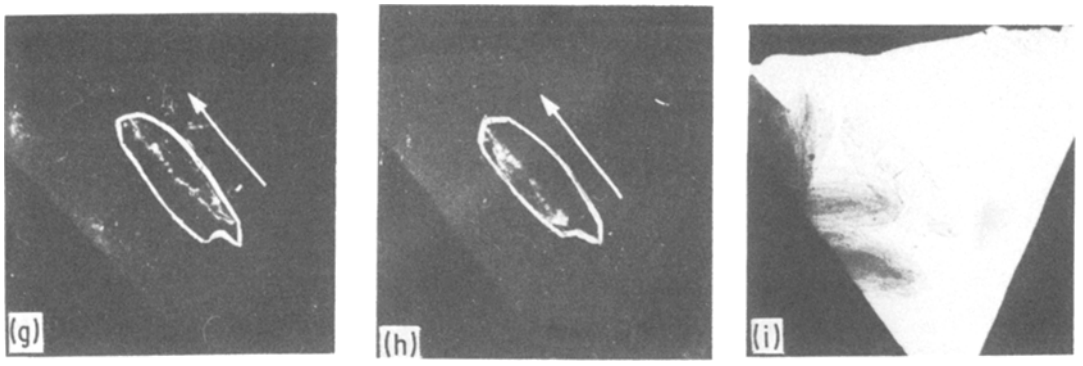

Figure 5 Continued.

process. This peak is reduced or removed if annealing is inhibited by crosslinking the crystal surface using radiation [9]. The two sharper peaks can be identified with the melting of the original crystals and indicate a two-stage process. This is strikingly confirmed in the electron micrographs. In Fig. 8a the {1 0 0} crystal sectors have melted out completely, while the {1 1 0} sectors remain intact apart from a small degree of melting around the crystal edge. Fig. 8b shows crystals which were heated to a slightly higher temperature, where the {1 1 0} sectors have also started to melt. In both cases, the ridged surface structure seen in areas of multilayer growth suggests that annealing has occurred there. The temperature to which the crystals were heated is not known precisely, but is in the range 122 to 128° C, which is in agreement with the position of the doublet in the DSC trace. The first of these peaks can be identified with the melting of the {1 0 0} sectors, and the second with the {1 1 0} sectors (as proposed by Harrison [10]).

The thermogram from the sample HTC105.6 shown in Fig. 9e has only two melting endothems.

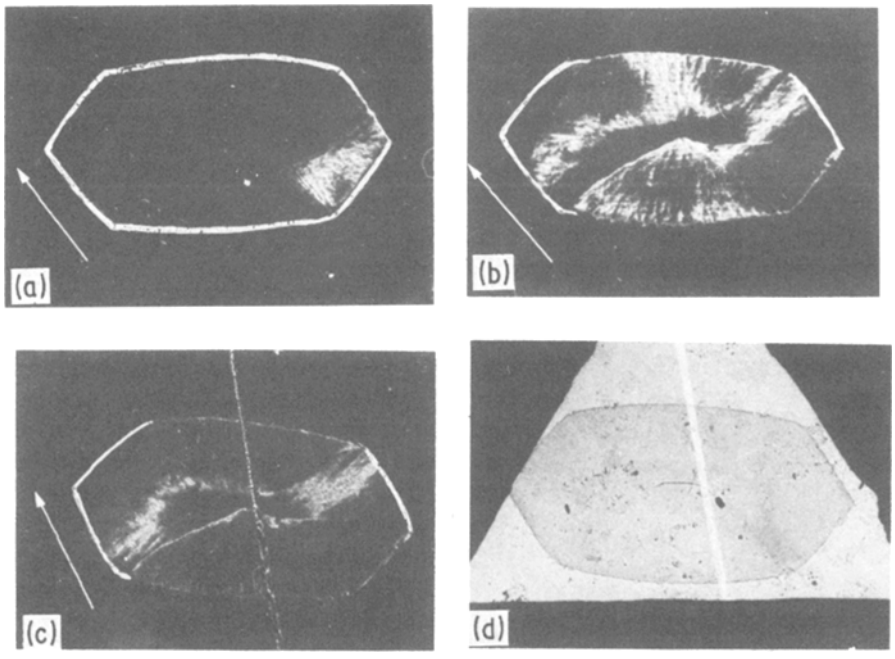

Figure 6 Dark- and bright-field electron micrographs of type B crystals. Tilting series with tilt axes as shown by arrows. (a) to (d) grown from hexatriacontane at 105.6° C. (e) to (h) grown from tetradecanol at 111.8° C. 1 1 0 imaging was used in both cases. Both crystals appeared uniformly dark for negative tilt values. The angles of tilt are as follows: (a) + 11°, (b) + 8°, (c) + 3°, (d) BF, (e) + 15°, (f) + 8°, (g) 0°, (h) BF. Crystal outlines have been added in white.

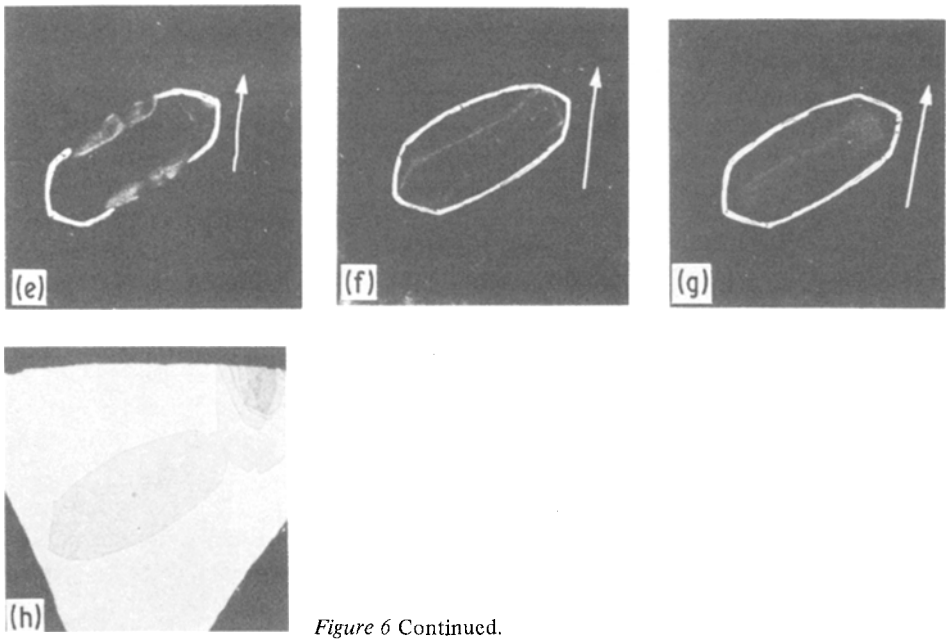

Figure 6 Continued.

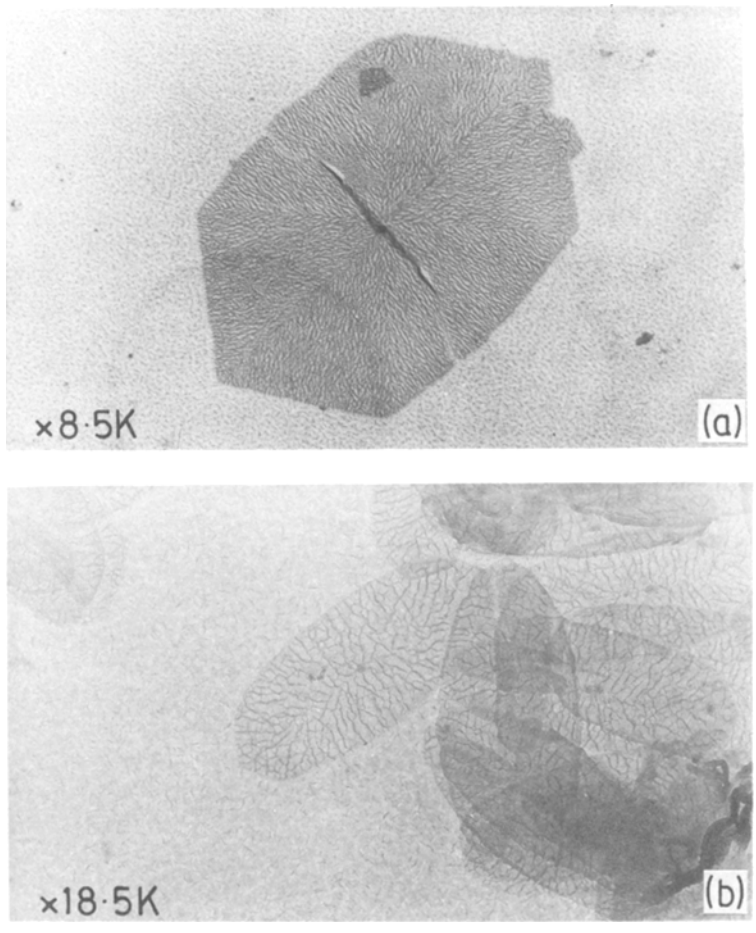

Figure 7 Crystals decorated with thermally degraded polyethylene and shadowed with Pt/Pd. (a) Crystal grown from octane at 95.8° C, (× 6.6 K) (b) Crystal grown from tetradecanol at 111.8° C, (× 14.1 K). Micrographs by courtesy of Mr. Boris Pretzel.

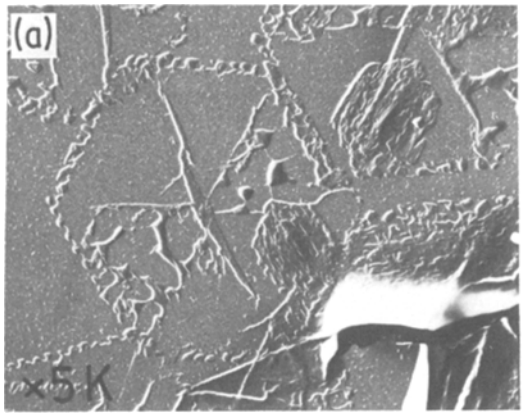

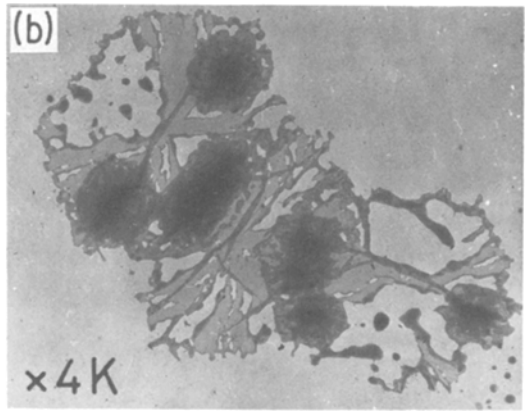

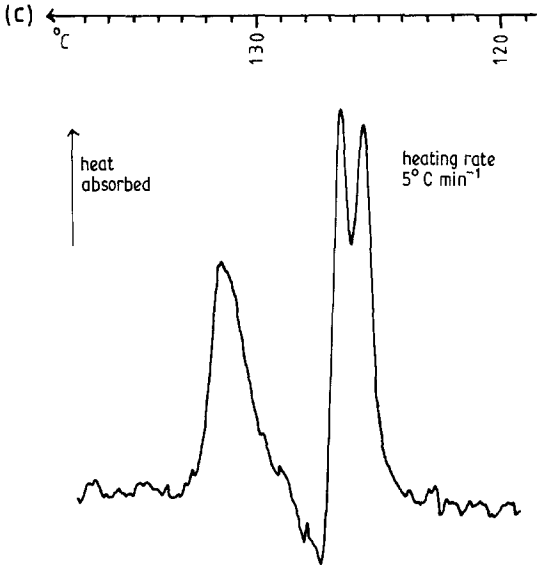

Figure 8 (a) and (b). Electron micrographs showing the melting behaviour of crystals grown from octane at 95° C. The crystals were heated to temperatures in the range 122 to 128° C. (a) is a replica shadowed with Pt/Pd, (c) the DSC thermogram for the same crystals, in suspension in silicone oil.

The first, fairly sharp peak, is at 125.0° C and can be identified as the melting point of the original crystals. The smaller and broader peak at approximately 130.0° C is again assumed to correspond to the melting of the annealed material. In the electron microscope, a variety of melting behaviours were revealed. Some examples are shown in Figs. 9a to d. The general trend is for melting to start in the {1 1 0} sectors and spread to the rest of the crystal, often leaving a rim around the crystal edge which shows some signs of having annealed. However, this behaviour is not universal and distinctions between the different crystal sectors are much less well-defined than in the previous case. Despite the differences in the degree of melting, all the crystals in Figs. 9a to d were held at the same temperature, 123.5° C, for the same length of time, so any difference in thermal stability between different areas of crystal must be very small. Some signs of annealing are apparent, mainly around the edges of melted areas, or where the crystal is multilayered (Fig. 9d).

For the sample EC107.0, the DSC trace again shows one distinct melting endotherm, which occurs at 126.9° C. This is shown in Fig. 10d. Small, ill-defined peaks occur at around 128.5° C and 130.5° C, which could correspond to the melting of annealed material. The micrographs, Figs. 10a to c, show no sign of preferential sector melting. Melting starts around the crystal edges and gradually progresses inwards. In many cases the area around the 1 1 0 crystal apex is the first to melt, but this is not universal. Areas adjacent to melted crystal show some signs of possible thickening, although this could be partly due to material which has recrystallised on cooling.

The results for TD111.8, shown in Fig. 11, are very similar. Again, only one clear melting endotherm is seen, at 126.7° C, with indications of a small amount of material melting at higher temperatures. Melting appears to proceed from the crystal edges inwards, with no clear distinction between different crystal sectors.

The sample HTC112.8, however, does show a double peak in the DSC trace, as seen in Fig. 12e. The main peak is at 128.4° C, with a shoulder at 128.0° C. There is no indication of further melting beyond this. The origin of this effect is not clear. Examination of the electron micrographs, Figs. 12a to d, shows that at early stages of melting the crystals behave in a similar manner to those of EC107.0 and TD111.8, with melting

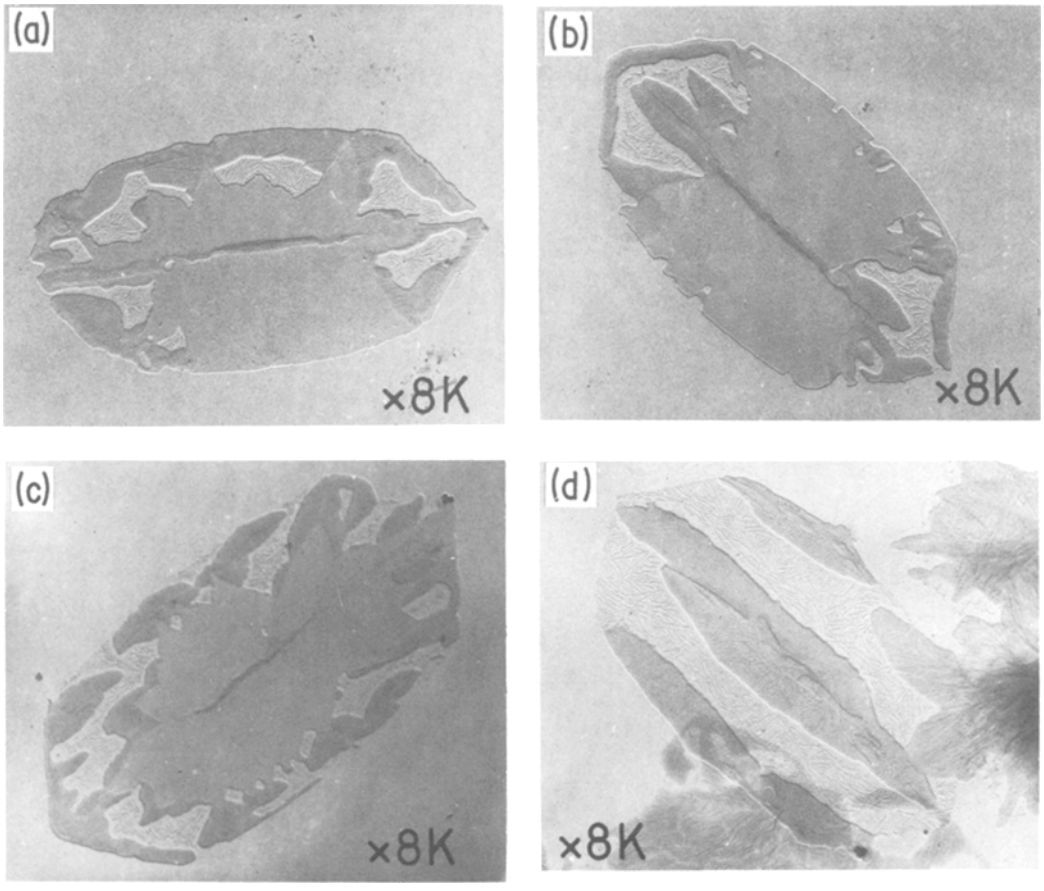

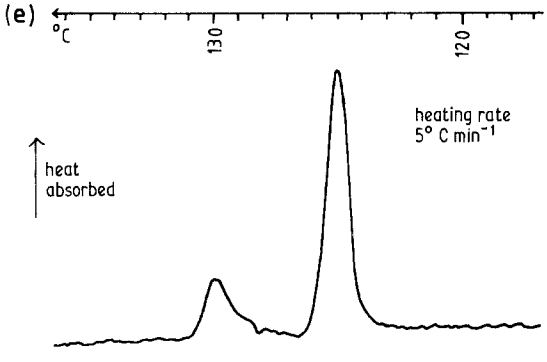

Figure 9 (a) to (d) Electron micrographs showing the melting behaviour of crystals grown from hexatriacontane at 105.6° C. The melting temperature was 123.5° C in all cases. All are shadowed with Pt/Pd. (e) The DSC thermogram for the same crystals, in suspension in silicone oil.

beginning at the crystal edges and progressing inwards. In this case the tendency for the apex area to melt first is quite pronounced, as can be seen from Fig. 12b. At higher temperatures some unusual effects are seen; the crystal surface appears highly ridged, and small holes appear. These effects are unlikely to be due to annealing, since no evidence is seen in the DSC trace and the other results suggest a reduced tendency for the more elongated crystals to anneal. From other related experiments (as discussed in Part 3 [11]) it appears that the sample HTC 112.8 contains a small amount of residual solvent – most probably trapped within the surface layer. This could explain the anomalous result found in this case.

4. Discussion and conclusion

Crystals with axial ratios between 1.60 and 3.00 were investigated. Two types of three-dimensional structure could be identified, analogous to the "hollow pyramid" and "chair" morphologies seen in lozenge shaped crystals grown at lower temperatures. In most cases the two types were present in roughly equal proportions, as was found when these crystals were first recognized [3]. However, in one preparation only "chair" crystals were seen.

From the dark field results is is clear that while some degree of sectorization is retained as the

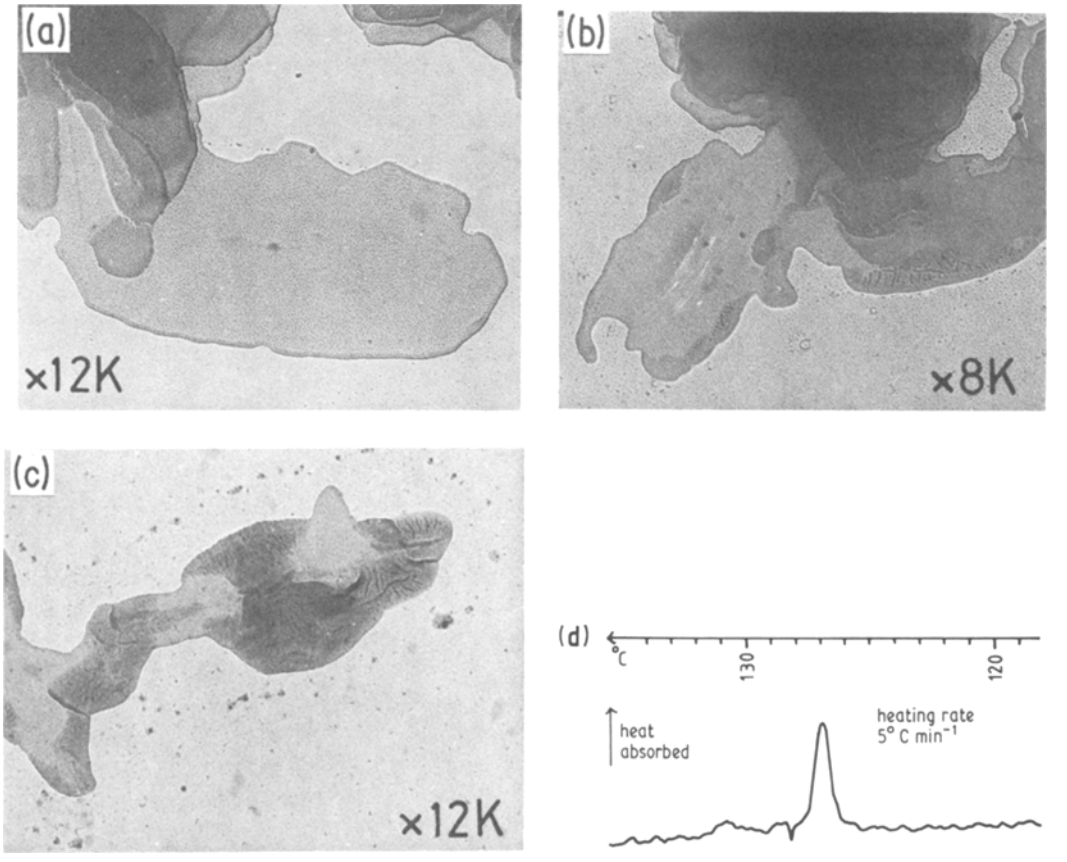

Figure 10 (a) to (c) Electron micrographs showing the melting behaviour of crystals grown from ethyl caproate at 107.0° C. The melting temperatures are (a) 126.5° C, (b) 127.0° C, (c) 128.0° C. (a) and (b) are shadowed with Pt/Pd. (d) The DSC thermogram for the same crystals, in suspension in silicone oil.

crystals become more elongated, the distinction between different sectors diminishes with increasing axial ratio. Crystals with low A/B values gave tilt angles similar to those seen by Bassett *et al.* [3]. In the most extreme case, crystals grown from hexatriacontane with $A/B = 3.00$ often showed only a discontinuity down the centre of the crystal, as reported by Keith [6]. The chair-type crystals in general showed a distinction between a central region of higher tilt running down the length of the crystal, with a gradual transition to two areas of lower tilt on either side. This type of crystal would produce the diffraction effects noted by Khoury and Bolz [7] and mentioned in the introduction. The existence of the chair-type morphology provides further evidence that at least some degree of sectorization remains as the crystals become more elongated and their faces more distinctly curved.

The results from the paraffin decoration substantiate these findings. Clearly defined sectors are seen in crystals with a low axial ratio. In more elongated crystals the sectors, while present, are less well-defined. The pattern of decoration within the "1 0 0" sectors of curved crystals suggests that the direction of growth is not strictly along [0 1 0], but rather along radial directions perpendicular to the curved crystal faces.

The remarkable feature of the melting effects is that they can identify sectorization in crystals where sectors are distinct. Calorimetry reveals multiple melting points which can then be identified with the melting of the different sectors seen in the microscope. This enables the sectorization to be characterized through thermal behaviour in the course of which several trends may be identified. Thus there is the disappearance of sector melting. The results of Harrison [10] for slightly truncated crystals ($A/B \simeq 1$) show a difference of 2.0° C between the melting points of the {1 0 0} and {1 1 0} sectors. For the sample O95.0, $A/B = 1.6$, this difference is reduced to 0.9° C. (Note the

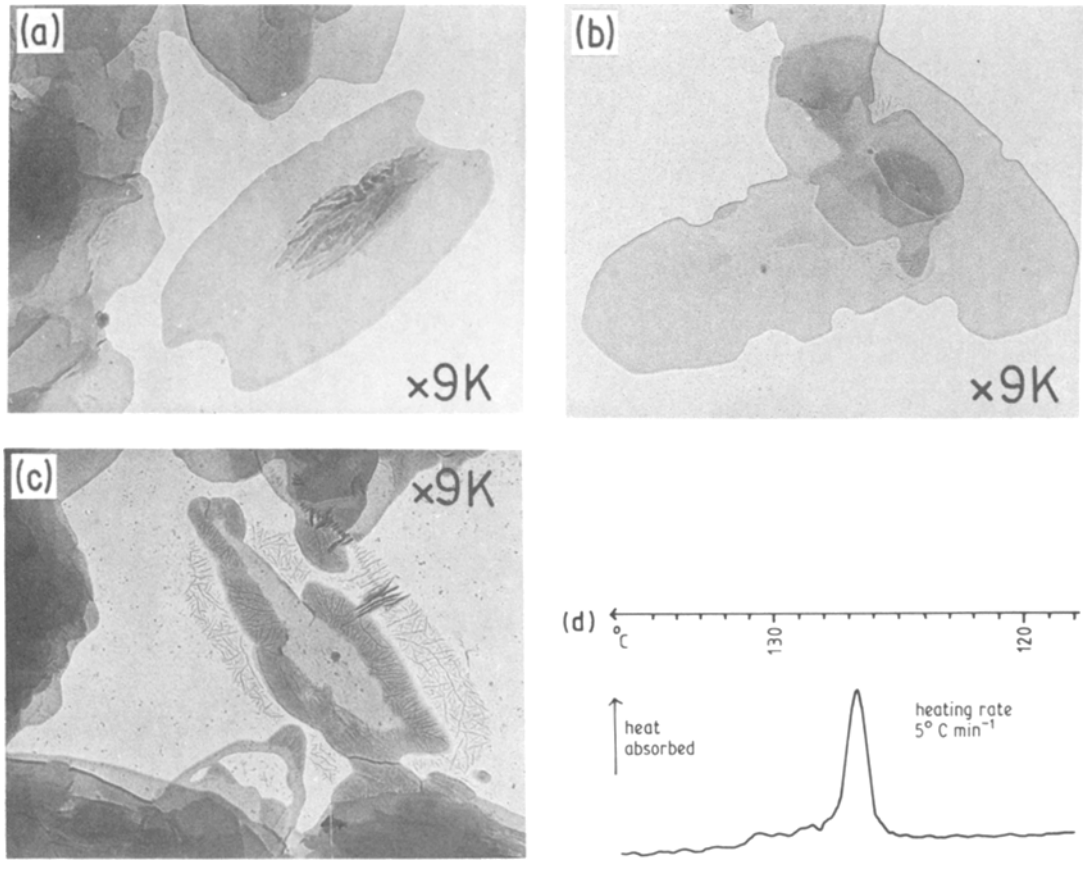

Figure 11 (a) to (c) Electron micrographs showing the melting behaviour of crystals grown from tetradecanol at 111.8° C. The melting temperatures are (a) 127.0° C, (b) 127.5° C, (c) 127.7° C (b) is shadowed with Pt/Pd. (d) The DSC thermogram for the same crystals, in suspension in silicone oil.

extreme sharpness of the melting peaks, quite unexpected for polymers!). In the more elongated crystals the effect is not seen at all. Rather, areas around the apices of the {1 1 0} faces appear to become marginally less stable. The melting temperature, T_m, of a polymer crystal of thickness l can be approximated by the equation

$$T_m = T_m^0 \left(1 - \frac{2\sigma_e}{l\Delta H}\right) \quad (1)$$

where T_m^0 is the equilibrium melting point of an infinite crystal, σ_e is the fold surface free energy, and ΔH is the specific heat of fusion [12]. Examination of this equation reveals that differences in melting temperature are likely to arise predominantly from differences in the value of the term $\sigma_e/l\Delta H$. Assuming ΔH to be constant within a particular crystal, the implication is that either the crystal thickness is greater in the {1 1 0} sectors, or the surface free energy is lower (or possibly a combination of these two factors), in crstals where the {1 0 0} sectors melt first. Possible differences in fold length between {1 1 0} and {1 0 0} sectors have recently been reported by Runt *et al.* [13] in studies of deconvoluted Raman spectra of polyethylene single crystals. However, these results suggest that the fold length may be longer in the {1 0 0} sectors, which would not explain the observed behaviour.

Another possibility is that the surface free energy is affected by different inter-stem distances. Using the unit-cell dimensions $a = 0.740$ nm $b = 0.493$ nm, for folding along {1 1 0} the stem separation is 0.445 nm, while for folding along {1 0 0} it is 0.493 nm. It is likely then that the folds in {1 0 0} sectors contain more monomer units than those in {1 1 0} sectors. If the strain per monomer is similar in the two cases, then the work of folding will be greater along {1 0 0}, leading to a higher surface free energy in the {1 0 0} sectors. Whatever

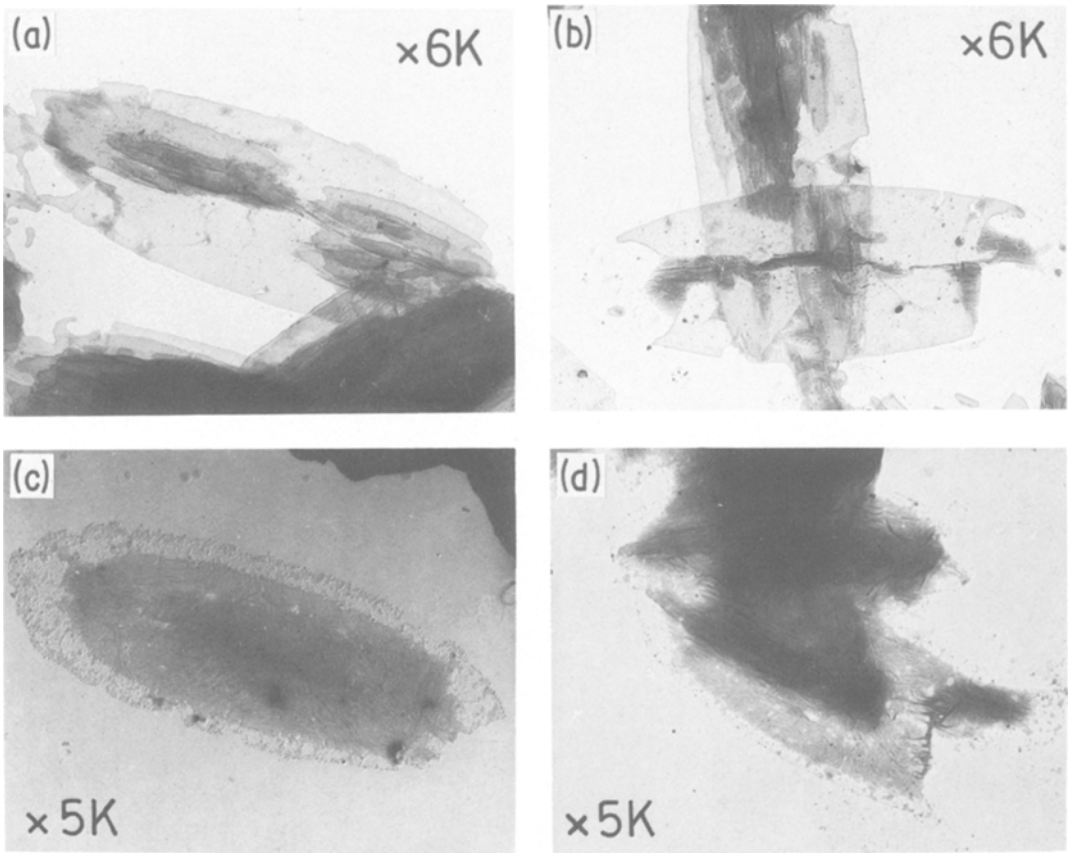

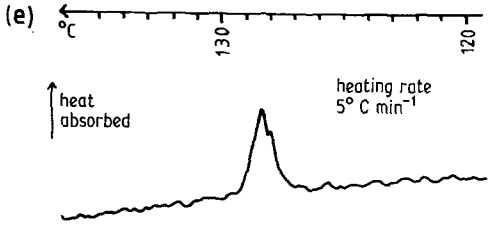

Figure 12 (a) to (d) Electron micrographs showing the melting behaviour of crystals grown from hexatriacontane at 112.8° C. The melting temperatures are (a) 128.0° C, (b) and (c) 129.0° C, (d) 129.5° C. (b) and (c) are shadowed with Pt/Pd. (e) The DSC thermogram for the same crystals, in suspension in silicone oil.

the explanation for the difference in melting points, the disappearance of the effect suggests that the sectors are becoming more similar as the axial ratio of the crystals increases – in agreement with the dark-field results.

The gradual reduction in size of the DSC peaks corresponding to the melting of annealed material is also interesting. This peak is highly pronounced in the sample O95.0, much smaller for HTC105.6, almost negligible for EC107.0 and TD111.8, and completely absent in the case of HTC112.8. The fold lengths of the crystals are expected to increase in this order (see Part 3 [11]) which would suggest that thicker crystals are less prone to anneal on heating. An alternative explanation is that the crystals grown at higher temperatures have already annealed during crystallization, and so are less likely to thicken further. This possibility will be investigated further in Part 3 of this series.

The tendency of crystals to melt at the edges and sharper corners, seen particularly in the samples EC107.0 and HTC112.8, could be due to local variations in the relative magnitude of the energy terms relating to the different surfaces. In Equation 1, contributions arising from side surface and edge free energies have been regarded as negligible and omitted. However, for molecules on or close to the crystal edges these terms may have a large influence, causing local reductions in dissolution temperature. The edges of thinner crystals are able to stabilise by thickening, thus counteracting the effect.

In Part 1 [1] the difficulty of explaining the

occurrence of curved morphologies within the framework of the kinetic theory was discussed. The gradual disappearance of distinct sectors as the crystallization temperature is raised throws further doubt on the applicability of the accepted model of chain folding along well-defined crystallographic directions under these conditions. The equalizaton of melting points within the crystals also suggests that the fold surface is becoming more uniform over the entire crystal implying the loss of the directionality associated with sectorization. Both these findings emphasize the need to consider modifications to the existing theory. The incorporation of some degree of surface roughening into the growth mechanism [14] provides one possible development.

It remains to be seen whether the fold lengths of curved crystals grown at high temperatures are in accordance with the predictions of the kinetic theory and whether any isothermal thickening takes place during their growth. These questions will be considered in Part 3 of this series.

Acknowledgement

We wish to acknowledge the assistance of Mr Boris Pretzel, who carried out the paraffin decoration experiment.

References

1. S. J. ORGAN and A. KELLER, *J. Mater. Sci.* **20** (1985) 1571.
2. J. C. WITTMAN and B. LOTZ, *Makromol. Chem. Rapid Commun.* **3** (1982) 733.
3. D. C. BASSETT, F. C. FRANK and A. KELLER, *Phil. Mag.* 8 (1973) 1753.
4. D. M. SADLER, Ph.D. Thesis, Bristol University (1969).
5. T. KAWAI and A. KELLER, *Phil. Mag.* **11** (1965) 1165.
6. H. D. KEITH, *J. Appl. Phys.* **35** (1965) 3115.
7. F. KHOURY and L. H. BOLZ, 38th Annual Proceedings of the Electron Microscopy Society of America by San Francisco, California, 1980, edited by G. W. Bailey.
8. G. A. BASSETT, D. J. BLUNDELL and A. KELLER, *J. Macromol. Sci. (Phys.)* **B1(1)** (1967) 161.
9. H. E. BAIR and R. SALOVEY, *J. Macromol. Sci.* **B3** (1969) 3.
10. I. R. HARRISON, *J. Polym. Sci. Polym. Phys. Ed.* **11** (1973) 991.
11. S. J. ORGAN and A. KELLER, *J. Mater. Sci.* **20** (1985) 1602.
12. J. I. LAURITZEN and J. D. HOFFMAN, *J. Res. Natl. Bur. Stand.* **64A** (1960) 73.
13. J. RUNT, I. R. HARRISON, W. D. VARNELL, and J. I. WANG, *J. Macromol. Sci. (Phys.)* **B22** (1983) 197.
14. D. M. SADLER, *Polymer.* **24** (1983) 1401.

Received 15 August
and accepted 13 September 1984